Bioelectromagnetics 41:63–72 (2020)

Perturbing Circadian Oscillations in an In Vitro Suprachiasmatic Nucleus With Magnetic Stimulation

Binyam T. Kassahun,[1] Martin Bier,[1]* and Jian Ding[2]

[1]Department of Physics, East Carolina University, Greenville, North Carolina
[2]Department of Physiology, Brody School of Medicine, East Carolina University, Greenville, North Carolina

Many neurological disorders are associated with abnormal oscillatory dynamics. The suprachiasmatic nucleus (SCN) is responsible for the timing and synchronization of physiological processes. We performed experiments on PERIOD2::LUCIFERASE transgenic "knock-in" mice. In these mice, a gene that is expressed in a circadian pattern is fused to an inserted gene that codes for luciferase, which is a bioluminescent enzyme. A one-time 3 min magnetic stimulation (MS) was applied to excised slices of the SCN. The MS consisted of a 50-mT field that was turned on and off 4,500 times. The rise time and fall time of the field were 75 μs. A photon count that extended over the full 5 days that the slice remained viable, subsequently revealed how the MS affected the circadian cycle. The MS was applied at points in the circadian cycle that correspond to either maximal or minimal bioluminescence. It was found that both the amplitude and period of the endogenous circadian oscillation are affected by MS and that the effects strongly depend on where in the circadian cycle the stimulation was applied. Our MS dose is in the same range as clinically applied doses, and our findings imply that transcranial MS may be instrumental in remedying disorders that originate in circadian rhythm abnormalities. Bioelectromagnetics. 2020;41:63–72.

Keywords: **suprachiasmatic nucleus slice; circadian rhythm; transcranial magnetic stimulation; PERIOD2::LUCIFERASE transgenic mice; bioluminescence recording**

INTRODUCTION

Body temperature, sleep, hormone levels, digestive activity, and many other physiological phenomena maintain a cycle of about 24 h in mammals, even in the absence of a light/dark cycle. When a light/dark cycle is present, the organism will generally synchronize its endogenous cycles with the environmental one. The suprachiasmatic nucleus (SCN) is the small specialized region within the hypothalamus where the periodicity is controlled and where the synchronization between the endogenous physiology and the external light/dark cycle takes place. It is a collection of about 20,000 neurons that synchronize with each other and ultimately generate a collective oscillation with a period of about 24 h [Pittendrigh and Daan, 1976]. The SCN is located close to where the two optic nerves cross. It is part of the cortex and receives input from other brain regions as well as from the optic nerves. It ultimately seeks to establish stable fixed phase-relationships between the environmental input and different physiological oscillations.

In the SCN, the expression of the PER2 protein follows a circadian pattern [Lowrey and Takahashi, 2011]. PER2 has been found to be one of the most important proteins involved in imposing a circadian rhythm on an organism [Ripperger and Albrecht, 2012]. Reporter genes have been a valuable experimental tool in the study of circadian oscillations [Yoo et al., 2004]. In the PERIOD2::LUCIFERASE transgenic knock-in mice, a firefly gene that codes for the enzyme luciferase was fused to the PER2 gene, leading to a PERIOD2::-LUCIFERASE fusion protein. Luciferase catalyzes the

Grant Sponsor: National Institute of Neurological Disorders and Stroke, grant number: NS-047014 (to J.M. Ding).

Conflict of interest: None.

*Correspondence to: Martin Bier, Department of Physics, East Carolina University, Greenville, NC 27858. E-mail: bierm@ecu.edu

Received for review 24 November 2018; Accepted 21 November 2019

DOI:10.1002/bem.22235
Published online 19 December 2019 in Wiley Online Library (wileyonlinelibrary.com).

production of oxyluciferin. Upon catalyzed conversion, the oxyluciferin is in an excited state. When oxyluciferin next goes to its ground state, a photon of green light is emitted. In the transgenic mice, the recorded bioluminescence is a measure of the quantity of the present PER2 [Yoo et al., 2004].

Previous studies have shown how the activity of the endogenous pacemaker, the SCN, can be analyzed in vitro in hypothalamic brain slices [Green and Gillette, 1982; Gillette, 1986; Gillette, 1991]. By doing a photon count on SCN slices of the aforementioned transgenic mice, one can follow the gene activity that is associated with the endogenous circadian rhythm. The monitoring of photons coming from luciferase activity does not require invasive action and can continue for about 4–5 days. In this way, gene oscillatory activity can actually also be observed on live, transgenic, luminescent, whole animals [Baker, 2010].

Transcranial magnetic stimulation (TMS) is a noninvasive technique in which time-varying magnetic fields are used to induce electric potentials and currents in parts of the brain. The technique is already commonly used in the treatment and diagnosis of various ailments [George et al., 1996; Dannon and Grunhaus, 2001; Gao et al., 2010; Smeal et al., 2010; Yang et al., 2010]. In animal experiments, TMS has been shown to affect memory [Li et al., 2007], synaptic plasticity [Ahmed and Wieraszko, 2006], and motor cortex function [Rotenberg et al., 2010]. Different cortical excitation and inhibition activity are observed depending on the frequency of TMS used. Generally, low frequency (<1.0 Hz) stimulation has inhibitory effects on cortical excitation [Chen et al., 1997], whereas high-frequency stimulation (>20 Hz) leads to an increase in cortical excitability [Pascual-Leone et al., 1998]. External stimulation, furthermore, appears to be able to restore an abnormally functioning cortex [Siebner and Rothwell, 2003; Devos and Defebvre, 2006]. Although studies have demonstrated the physiological effects of TMS, there has been limited research on how TMS impacts the underlying biochemistry of the circadian rhythm.

The bioluminescence oscillation of our excised SCN slices follows circadian time (CT). The CT scale is an emergent and endogenous one that is particular to the individual brain slice. The conventional clock time is "Zeitgeber time" (ZT). In the natural environment, the imposed light/dark ZT cycle entrains the CT cycle. We take SCN slices from mice that have been accustomed to a 24 h cycle with 12 h of light followed by 12 h of darkness. ZT 0 corresponds to the time of the day when the lights get turned on. ZT 12 corresponds to the time of the day that the lights get turned off. It is at nightfall, around ZT 12, that the mice are most active, and when we observed a bioluminescence maximum in the subsequently excised SCN slices. In our experiments, we applied a one-time magnetic stimulation (MS) to the slice. Within 5 min, we administered 9,000 short pulses. These pulses were applied either at the first bioluminescence minimum (at ZT 0) after extraction of the slice or at the bioluminescence maximum (at ZT 12) after this minimum.

TMS can be applied to an in vivo brain. However, the SCN is in that case surrounded by other electrically conducting tissue, which makes it hard to estimate and control the dose of magnetically induced current in the SCN. With TMS, it is furthermore impossible to focus the MS exclusively on the SCN and to not also possibly stimulate other brain tissue. Working with isolated SCN slices guarantees specificity [Bier and Weaver, 2018].

The SCN is the engine behind an organism's circadian rhythm. The bioluminescence measurements on SCN slices allow us to noninvasively and quantitatively record the circadian oscillations. The aim of this work is to determine, on the gene expression level, whether or not MS has an effect on the circadian oscillator. Can MS affect the amplitude of the circadian oscillation? And can it delay or advance the occurrence of the next extremum in the circadian cycle?

MATERIALS AND METHODS

Animals

Animal studies were conducted in compliance with the Animal Welfare Act and Public Health Service Guidelines. The protocol was approved by East Carolina University's Animal Care and Use Committee (AUP #Q201b).

SCN tissues were obtained from adult, male (8–12 weeks old, $n = 45$), homozygous PER2::LUCIFERASE (PER2::LUC) transgenic knock-in mice [Yoo et al., 2004]. The mice were housed under a 12 h light (500 lux)–12 h dark (<0.1 lux) cycle. All animals were kept in individual cages that were equipped with running wheels. Prior to the experimental procedures, wheel-running activity was monitored for 4 weeks using ClockLab data acquisition software (Actimetrics, Evanston, IL) to ensure that animal behavior was entrained to the light-dark cycle. The actogram (Fig. 1) shows that such entrainment was indeed the case.

Brain Slice Procedure

In this preparation, the SCN was isolated from other brain regions so that it could be subjected to MS.

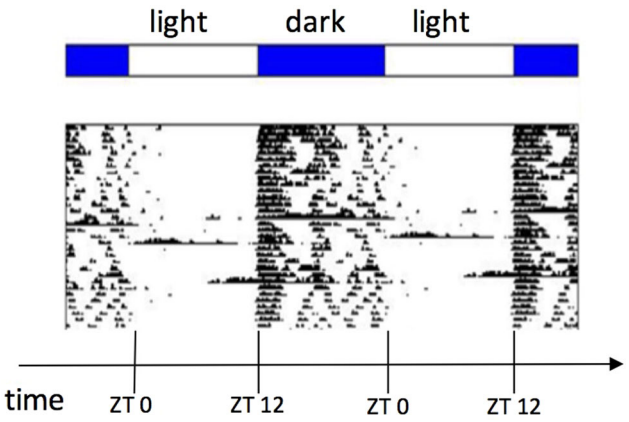

Fig. 1. An actogram to show that, prior to experimental procedures, the PER2::LUC mice exhibited a 24 h cycle in their wheel-running activity. The white and blue colors on the top bar indicate the externally imposed light and dark, respectively. Below, the wheel-running intensity is represented by the height of the vertical black bar, where each horizontal line stands for a different animal. Wheel running appears most intense right after the onset of darkness.

Before the slicing began, the surgical tools were prepared and autoclaved. Mouse transfer and cutting procedures were done during the light-on hours (ZT 8–10) to minimize preparation-induced phase shifts [Yoshikawa et al., 2005]. Mice were anesthetized with isoflurane and, before decapitation, the absence of pain reflexes was ascertained. The skull was removed using autoclaved surgical tools. After the brain was isolated, it was placed in cold Hanks' balanced salt solution (HBSS; Sigma-Aldrich, St. Louis, MO) for roughly 1 min to harden the tissue for the sectioning procedure. Subsequently, the tissue was fixed to a vibratome cutting platform (Leica Biosystems, Buffalo Grove, IL). There, a vibrating razor cut the tissue until the SCN location was reached. The SCN is shaped like a disk and has a diameter of roughly 0.7 mm [Paxinos and Franklin, 2004]. A slice with a thickness of 250 μm was cut from the SCN. From each SCN, just one slice was taken for further culturing and experimentation. During cutting and sectioning, the sample was submerged in Hanks' buffered salt solution. Hanks' buffered salt solution is obtained by adding HEPES, NaHCO3, penicillin, and streptomycin to HBSS, as described in table 1 of Yamazaki et al. [2000]. A pH of 7.1 was maintained.

Tissue Cultures

Techniques for culturing organotypic SCN slices on a culture membrane were adopted from earlier studies [Stoppini et al., 1991; Yamazaki et al., 2000; Savelyev et al., 2011]. A 0.1 M stock solution of Beetle Luciferin (Promega, Madison, WI) was prepared prior to sectioning and stored in a freezer with a light-tight seal. A culture medium with 0.1 mM luciferin was obtained by dissolving 10 μl luciferin in 10 ml of the culture medium. After sectioning was complete, the SCN tissue was transferred onto a 35 mm Millipore Petri dish containing a 0.4 μm pore size culture membrane (Millipore, Bedford, MA), and 1,400 μl of the luciferin-containing culture medium.

The culture medium was prepared using: 10.0 g of Dulbecco's modified Eagle's medium (DMEM) low glucose powder without sodium bicarbonate and without phenol red (#D-2902; Sigma-Aldrich), 2.5 ml Penicillin–Streptomycin (#15140-122, 10,000 U/ml; Thermo Fisher Scientific, Waltham, MA), 20 ml B27 supplement (50×)-serum free (#17504-044; Thermo Fisher Scientific), 4.7 ml of Sodium Bicarbonate ($NaHCO_3$) 7.5% solution (#25080-094; Thermo Fisher Scientific), 10 ml HEPES 1 M Solution (#H0887; Sigma-Aldrich), and 3.5 g D-glucose powder (#G7021; Sigma-Aldrich). All substances were dissolved in sterile water (autoclaved Milli-Q water) and the total volume was adjusted to 1 L. We again followed the guidelines of Yamazaki et al. [2000] in the preparation of the medium. The pH of the final medium was adjusted to 7.2 using HCl (to decrease the pH) and NaOH (to increase the pH). Finally, the culture medium was filtered using a Corning 500 ml vacuum filter/storage bottle system (# 431097; Corning, Corning, NY) with a 0.22 μm pore size and a 33.2 cm^2 polyethersulfone (PES) membrane. The medium was protected from light and stored at 4°C. The Petri dish containing the SCN, culture medium/membrane, and luciferin was sealed with a 40 mm cover glass (#102240; Thermo Fisher Scientific) and high-vacuum silicone grease (#Z-273554; Sigma-Aldrich), and then transferred to a bioluminescence detector.

Bioluminescence Recording

Luciferase catalyzes a conversion of luciferin that ultimately leads to the emission of a green photon. The emitted photons from an SCN slice were counted with photon-counting photomultiplier-tubes (PMT). Luminescence was recorded using a 32-channel LumiCycle luminometer (Actimetrics) [Welsh et al., 2004]. The luminometer was inside an Isotemp incubator (Fisher Scientific, Hampton, NH) that was kept at 36 °C. At 37 °C, this incubator has a temperature uniformity of ±1 °C. The body of the incubator and

the door were electrically connected with a ground wire to eliminate electrical noise. A multimeter was used to verify that the electrical circuitry functioned properly. A previous study has shown that the maximum magnetic field generated by the heating units and control circuits inside the incubator was 1.85 μT with a maximum background magnetic field of 0.32 μT [Dong and Heroux, 2012]. Such fields are negligible compared to, for instance, the Earth's permanent magnetic field. The Lumicycle has an internal fan. That fan circulated incubator air to maintain a temperature of 36 °C within the chamber.

The luminometer has 4 PMTs and an automated turntable that moves the samples so data can be taken from up to 32 slices at the same time. The PMTs are specially designed to detect low dark counts in the green part of the spectrum. The bioluminescence (counts/min) was plotted as a function of time (Fig. 2). To give the system time to equilibrate, we started data collection 12 h after the samples were placed in the luminometer.

Electrophysiological measurements were not conducted for this study. Slice viability was checked by evaluating the highest and lowest PER2::LUC expression in the first cycle. If the peak expression level corresponded to ZT 12 and the lowest expression level corresponded to ZT 0, then the slice was deemed viable.

Magnetic Stimulation

For the one-time application of the MS, the Petri dishes containing the SCN tissues were transferred from the Lumicycle chamber to be placed into another Isotemp incubator with a matching temperature setting (36 °C). The control samples were also removed from the Lumicycle and subjected to sham treatment under the same experimental condition. Both control and exposed samples were returned to their respective locations within the Lumicycle chamber after exposure/sham treatments were completed. Initially, we did sham treatments both at a bioluminescence minimum and at a maximum. As we noticed no difference between these two groups, the sham treatments that were used to generate the control data for the figures were all performed at a bioluminescence maximum.

Samples were stimulated either at ZT 0 (trough stimulation) or at ZT 12 (peak stimulation). To administer the MS, the 35 mm Petri dish containing the SCN sample was placed on a thin (1 mm) flat microscope slide. The glass slide was then attached to a test tube clamp and placed over a coil. A retort stand (ring stand) was used to support the test tube clamp. The stimulating coil had 5 layers with 37 windings each and was placed 1.0 cm above the sample with the windings in the horizontal plane. The inner radius of the coil was 2.5 cm. The diameter of the wire was 0.7 mm. The inductance of the coil was 1.2 mH.

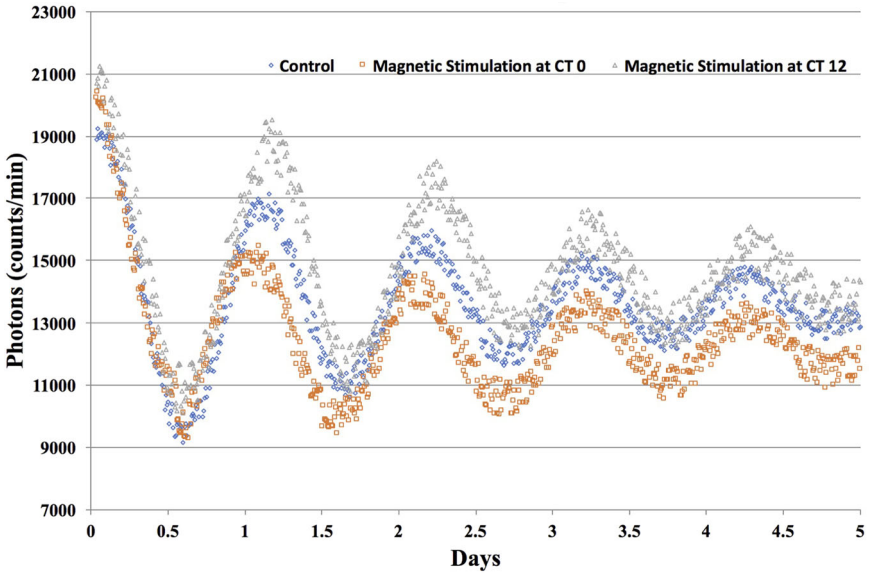

Fig. 2. Bioluminescence recordings from three individual cultured suprachiasmatic nucleus slices. The blue diamonds are from a slice that received no stimulation. The gray triangles derive from a slice that received magnetic stimulation at the first peak (ZT 12, about 1 day after the slice was cut). The orange squares derive from a slice that received magnetic stimulation at the first trough (ZT 0, about 1/2 a day after the slice was cut).

Pulses from the MS unit were timed with a 555 timer IC. Each pulse was generated by the discharge of a 1,000 μF capacitor and had a duration of 200 μs with a current rise time as well as a current fall time of 75 μs. A maximal current of 6 A passed through the coil. Pulses were delivered at a frequency of 25 Hz. The MS procedure lasted 5 min. Within that 5 min window, the sample would be stimulated for 1 min followed by a 1 min pause, thus totaling 2 min of pause and 3 min of stimulation. During a minute of stimulation, the magnetic field changed 3,000 times, leading to a 5 min total of 9,000 electric pulses.

Using the standard formulae for the magnetic field ($B = \mu NI/l$, where μ is the magnetic permeability of the vacuum, N is the winding number, I is the current, and l is the coil's length) and the inductance of a solenoid ($L = \mu N^2 A/l$, where A is the cross-sectional area of the inside of the coil), it is readily derived from the numbers given in the previous paragraph that a maximal magnetic field B of about 50 mT was produced at the site of stimulation. With the rise/fall time of 75 μs, this implies $dB/dt \approx 700$ T/s. The induced electric field is proportional to dB/dt. Our values of B and dB/dt were in the same range as those in other experiments involving MS of rodent brains [Grehl et al., 2016; Tang et al., 2018]. The SCN slice with its surrounding tissue had a radius of about 2 mm. The diameter of the coil is much larger than the diameter of the slice and thus, as in the reference by Grehl et al. [2016], the magnetic field can be taken to be uniform inside the tissue. Applying Faraday's Law of Induction ($A \times dB/dt = -V_{ind}$, where A is the area of the slice), we derive a magnetically induced electric voltage, V_{ind}, of about 10 mV driving current around the sample. Our rise/fall time of 75 μs gives intracellular and extracellular ions sufficient opportunity to move and balance out the induced electric field [Bier and Weaver, 2018]. All of the imposed 10 mV will thus be distributed over the nonconducting cell membranes. This voltage is too small to directly trigger action potentials. Nevertheless, with setups very similar to ours, it has been found that such low-intensity repetitive MS is able to lower the action potential threshold and increase spike firing [Tang et al., 2016].

Three luminescence recordings are shown in Figure 2. The 0 days point where the graph starts corresponds to the ZT 12 maximum that occurs 2–4 h after the cutting.

Fifteen slices received the stimulation at ZT 0, when the photon count was minimal (trough stimulation at ½ days; orange squares in Fig. 2). Fifteen slices received the stimulation at ZT 12, when the photon count was maximal (peak stimulation at day 1; gray triangles in Fig. 2). Finally, fifteen slices never received stimulation and functioned as a control (control; blue diamonds in Fig. 2).

Data Processing

To assess the effects of the stimulation, we performed a Rayleigh analysis [Batschelet, 1981] using Oriana Software (Kovach Computing Services, Pentraeth, UK). Figures 3 and 4 are Rayleigh plots for trough stimulation (at ZT 0) and for peak stimulation (at ZT 12), respectively. The outer circle represents the 24 h ZT cycle. For Figures 3 and 4, the blue dots indicate where bioluminescence minima and maxima occurred, respectively. By drawing vectors from the origin to each of the blue dots and next taking the average of these fifteen vectors, the black vector in the graph was obtained. Ultimately, the length r of this average vector is a measure for the degree of synchronization. The direction of the black vector, furthermore, indicates the average phase.

Figure 5 shows group-averaged photon counts for all three groups (control, peak stimulation, trough stimulation). The depicted photon count for each group is an average over three subsequent peaks.

RESULTS AND DISCUSSION

Figures 2–5 sum up the results of our study. The MS has an effect and the point in the circadian cycle at which the MS is administered appears to be essential. When the stimulation is applied at a PER2-expression *minimum*, the results are (i) an average increase of the next circadian period by 2.47 ± 0.38 h ($P < 0.001$; Student's t test, $n = 15$) compared with the control, (ii) a wider distribution for these circadian periods, i.e., the addition of a random factor to the period, and (iii) an overall decrease of PER2 expression by 17% ($P < 0.001$; Student's t test, $n = 15$). When the stimulation is applied at a PER2-expression *maximum*, the results are (i) an average shortening of the next circadian period by 1.46 ± 0.22 h ($P < 0.001$; Student's t test, $n = 15$) compared with the control, (ii) a narrower distribution of these circadian periods, and (iii) an overall increase of PER2 expression by about 22% ($P < 0.001$; Student's t test, $n = 15$).

As was mentioned in the Materials and Methods section, the induced transmembrane voltages by the MS are too tiny to directly trigger action potentials in excitable cells. Nevertheless, the one-time MS of just 5 min is sufficient to lead to measurable effects. The underlying mechanism behind the effect is mostly a matter of speculation. A possible explanation is that the induced voltages temporarily contribute to transmembrane

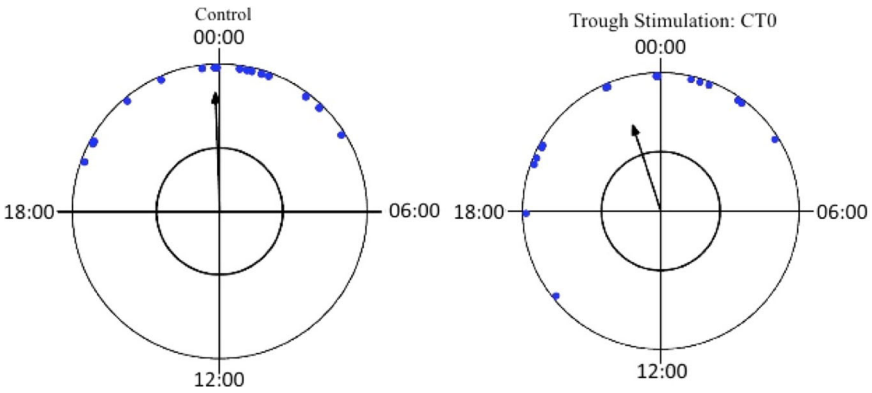

Fig. 3. A comparison of the control group (left) and the trough (ZT 0) stimulation group (right). A dot indicates the phase of the second minimum on the ZT scale. Stimulation occurs at the first minimum (cf. Fig. 2, at Day 1/2). The figure on the left represents the results for the control group. Without stimulation, we have $r = 0.81$ for the degree of synchronization. With stimulation, we have $r = 0.67$. So the stimulation desynchronizes the circadian rhythms and leads to a wider distribution of phases. The phase difference between the two black arrows, furthermore, indicates that stimulation extends the circadian period by 2.47 h (standard deviation 0.38, $P < 0.001$; Student's t test, $n = 15$).

voltages at the postsynaptic end of synaptic junctions, that these altered transmembrane voltages affect the probability of the occurrence of action potentials, and that longer-term effects next ensue. It is also possible that changes in PER2 expression resulted from an elevation in intracellular calcium in response to low-intensity MS [Grehl et al., 2015].

An oscillation invariably sets up a challenge to a physicist. The problem is to find the underlying dynamics, i.e., the mathematical how and why behind the period and amplitude. Endogenously generated oscillations in biological systems are generally more complicated than simple, linear, harmonic oscillators. They commonly appear to be limit cycle oscillations [Glass and Mackey, 1998]. Nature's choice for limit cycle oscillations is a sensible one. Limit cycles are robust, i.e., they persist with roughly the same amplitude and period in the presence of noise or small perturbations. Information about the underlying dynamics behind a limit-cycle oscillation can oftentimes be obtained by applying a pulse-like perturbation and observing how the system next relaxes back to the regular cycle.

This idea was first applied already 150 years ago when it was investigated how the respiratory

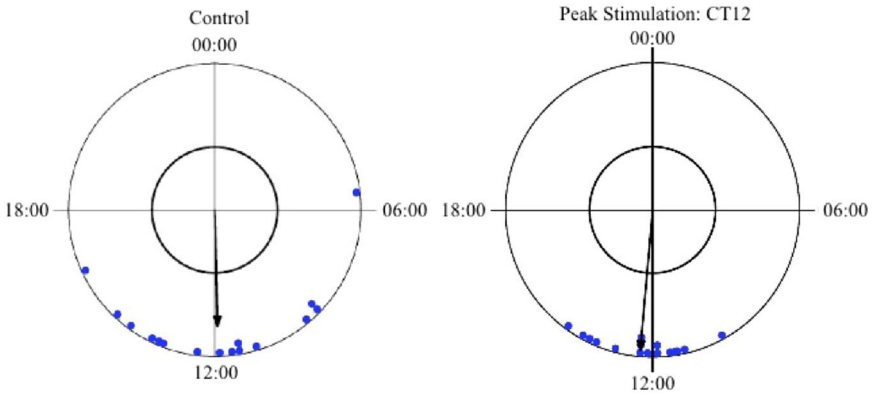

Fig. 4. A comparison of the control group (left) and the peak (ZT 12) stimulation group (right). A dot indicates the phase of the second maximum on the ZT scale (at around Day 2). Stimulation occurs at the maximum on Day 1 in Fig. 2. The figure on the left represents the results for the control group. Without stimulation, we have $r = 0.80$ for the degree of synchronization. With stimulation, we have $r = 0.95$. So the stimulation synchronizes circadian rhythms and leads to a narrower distribution of phases. The phase difference between the two black arrows, furthermore, indicates that stimulation shortens the circadian period by 1.46 h (standard deviation 0.22, $P < 0.001$; Student's t test, $n = 15$).

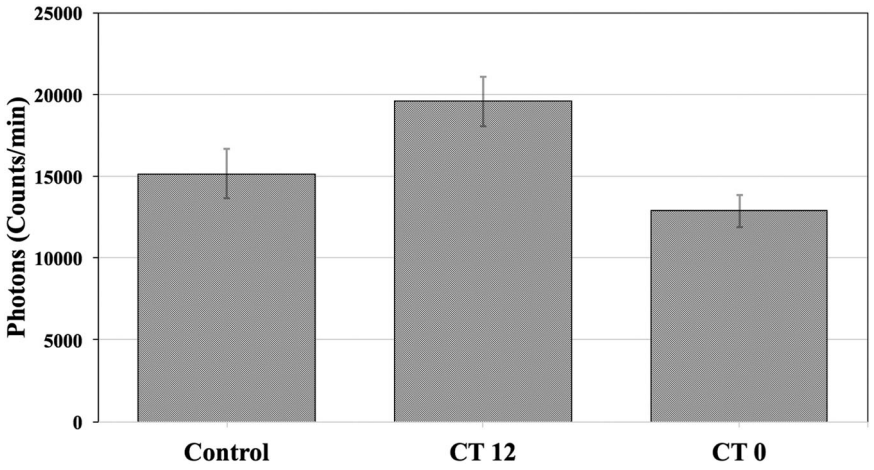

Fig. 5. The average photon count of three subsequent peaks. For each of the three bars, the average of all 15 slices in the group was taken. For the unstimulated control group and the ZT 0 group (trough stimulation), the first of the three pertinent peaks was the one at around 1 day. For the ZT 12 group (peak stimulation), the first of the three peaks over which the average was taken was the peak at around 2 days (cf. Fig. 2). The average photon count and the standard deviation are: 15,163 (±1493) for the control group, 19,578 (±1,523) for the ZT 12 group, and 12,903 (±983) for the ZT 0 group. What can already be inferred from Figure 2 is made more rigorous and quantitative in this figure: trough stimulation leads to stronger damping of the periodic signal and peak stimulation reduces the damping.

cycle reacted to sudden lung inflation [Breuer, 1868]. The outcome is not hard to understand. When applied during inhalation, the inflationary pulse shortens the period of the cycle. When applied during exhalation, the inflationary pulse extends the period of the cycle. Similar results ensued when mastication, locomotion, and Parkinsonian tremors were researched with this approach [Glass and Mackey, 1998]. It has been persistently found that the phase of the oscillation at the moment that the pulse is applied is crucial and determines whether a period is shortened or extended.

It is therefore not surprising when we find that the effect of MS on amplitude and period depends on whether the MS is applied during a maximum or a minimum. What is perhaps surprising and unusual is that the effect of the MS extends to beyond the period during which it was applied (cf. Fig. 2). In this sense, the MS of the SCN appears to resemble the resetting of the cardiac cycle by defibrillation or cardioversion.

The results obtained for MS applied at a PER2-expression maximum are of particular interest and may be of clinical significance. These results suggest that it may be possible to use a short application of TMS to restore to normality an SCN that produces weak signals. Such restoration could conceivably help patients with compromised circadian rhythms.

Our findings are consistent with what other researchers have found with a variety of methods. The modulation of cortical excitability can be studied by examining to what extent the cortical neurons synchronize their firing under different circumstances [Vyazovskiy et al., 2009]. A circadian dependency of neuronal excitability and synaptic functionality in the cortex has been established [Frank and Cantera, 2014]. Altered cortical excitability is associated with epilepsy [Kimiskidis et al., 2015], stroke [Huynh et al., 2016], depression [Bunse et al., 2014; Canali et al., 2014], and insomnia [van der Werf et al., 2010]. The circadian phase plays a critical role in modulating neuronal excitation and inhibition by potentially changing synaptic structure in humans [Frank, 2012].

In humans, TMS has been used to perturb non-REM sleep patterns. TMS exposure can also trigger endogenous slow oscillation and enhance sleep slow-wave activity [Massimini et al., 2007]. TMS application leads to a larger increase in spindle activity when administered during the depolarization phase (neurons silent) as compared to the hyperpolarization phase (neurons active) of the endogenous slow oscillation [Bergmann et al., 2012]. To what extent the cortical excitability is affected by TMS depends strongly on the circadian phase at the time of administration [Ly et al., 2016]. All these findings demonstrate that an appropriately timed MS can potentially restore abnormal cortical activity.

The coils in clinical TMS generally produce fields of about 1 T and pulses that last about a

millisecond [Rossini et al., 2015]. Such powerful coils are necessary because the targeted region inside the brain may be up to 5 cm away from the coils where the field is much weaker. It is through numerical simulation that estimates can be obtained of electromagnetic field strengths inside the brain during the application of TMS to a patient. Extensive simulations involving a model of a human head in silico have shown that the magnetic field at a target area 5 cm away from the coil is about 10% of the field at the coil [Lu and Ueno, 2017]. The latter reference used a frequency of about 2.5 kHz, i.e., a period of 400 μs. If we let the magnetic field change from −100 to 100 mT in the course of half a period, then we derive a rate of change of the magnetic field of $dB/dt \approx 1{,}000$ T/s. As was mentioned before, the induced electric voltage is proportional to the rate of change of the magnetic field and to geometrical factors. The 1,000 T/s is comparable to what was applied to the slices in our experiments. As magnetic fields cannot be sharply focused, it is impossible with TMS to target a well-defined signal at just a specific part of the human brain. The methods used to assess TMS effects in humans have traditionally involved analysis of EEG recordings or the interpretation of MRI or PET images [Siebner et al., 2009; Rossini et al., 2015]. We used SCN slices, custom MS techniques, genetically augmented mice, and advanced imaging tools. We thus achieved specificity and provided anatomic and physiological detail on the effect of MS on cortical activity.

Ultimately, our work could be instrumental in coming to a better understanding of the relation between perturbed environmental interactions and internal oscillatory pattern changes. Studies to understand perturbed states of cognition have mainly focused on how psychiatric disorders lead to a perturbed circadian rhythm [Bunse et al., 2014; Canali et al., 2014]. Implicit in these studies is the assumption that the psychiatric condition leads to a malfunctioning of the circadian clockwork. However, given the fact that tissues and organs receive their timing cues from the SCN, it is possible that an endogenous loss of phase coherence underlies the observed psychiatric disorders. By the time perturbed phase coherence becomes apparent in daily actions, it has propagated through many networks. TMS could help researchers in understanding the role of the SCN in neurological disorders, and it could possibly play a role in preventing or remedying such disorders.

REFERENCES

Ahmed Z, Wieraszko A. 2006. Modulation of learning and hippocampal, neuronal plasticity by repetitive transcranial magnetic stimulation (RTMS). Bioelectromagnetics 27:288–294.

Baker M. 2010. Whole-animal imaging: The whole picture. Nature 463:977–980.

Batschelet E. 1981. Circular Statistics in Biology. New York, NY: Academic Press. pp 54–58.

Bergmann TO, Mölle M, Schmidt MA, Lindner C, Marshall L, Born J, Siebner HR. 2012. EEG-guided transcranial magnetic stimulation reveals rapid shifts in motor cortical excitability during the human sleep slow oscillation. J Neurosci 32:243–253.

Bier M, Weaver JC. 2018. Signals, noise, and thresholds. In: Greenebaum B, Barnes F, editors, Bioengeneering and Biophysical Aspects of Electromagnetic Fields, 4th ed. Boca Raton, FL: CRC Press. pp 261–297.

Breuer J 1868. Die Selbststeuerung der Athmung durch den Nervus vagus. Sitzungsberichte der kaiserlichen Akademie der Wissenschaften Wien 58:909–937 (in German). Translated by Ullman E. 1970. In: Porter R, editor. Breathing: Hering-Breuer Centenary Symposium. London: J&A Churchill. pp 365–394.

Bunse T, Wobrock T, Strube W, Padberg F, Palm U, Falkai P, Hasan A. 2014. Motor cortical excitability assessed by transcranial magnetic stimulation in psychiatric disorders: A systematic review. Brain Stimul 7:158–169.

Canali P, Sferrazza Papa G, Casali AG, Schiena G, Fecchio M, Pigorini A, Smeraldi E, Colombo C, Benedetti F. 2014. Changes of cortical excitability as markers of antidepressant response in bipolar depression: Preliminary data obtained by combining transcranial magnetic stimulation (TMS) and electroencephalography (EEG). Bipolar Disord 16:809–819.

Chen R, Classen J, Gerloff C, Celnik P, Wassermann E, Hallett M, Cohen L. 1997. Depression of motor cortex excitability by low-frequency transcranial magnetic stimulation. Neurology 48:1398–1403.

Dannon PN, Grunhaus L. 2001. Effect of electroconvulsive therapy in repetitive transcranial magnetic stimulation nonresponder MDD patients: A preliminary study. Int J Neuropsychopharmacol 4:265–268.

Devos D, Defebvre L. 2006. Effect of deep brain stimulation and L-dopa on electrocortical rhythms related to movement in Parkinson's disease. Prog Brain Res 159:331–349.

Dong S, Heroux P. 2012. Survey of extra-low frequency and very-low frequency magnetic fields in cell culture incubators. arXiv 1211:2458. [q-bio.QM].

Frank MG. 2012. Erasing synapses in sleep: Is it time to be shy? Neural Plast 2012:264378.

Frank MG, Cantera R. 2014. Sleep, clocks, and synaptic plasticity. Trends Neurosci 37:491–501.

Gao F, Wang S, Guo Y, Wang J, Lou M, Wu J, Ding M, Tian M, Zhang H. 2010. Protective effects of repetitive transcranial magnetic stimulation in a rat model of transient cerebral ischaemia: A micropet study. Eur J Nucl Med Mol Imaging 37:954–961.

George MS, Wassermann EM, Williams WA, Steppel J, Pascual-Leone A, Basser P, Hallett M, Post RM. 1996. Changes in mood and hormone levels after rapid-rate transcranial magnetic stimulation (RTMS) of the prefrontal cortex. J Neuropsychiatry Clin Neurosci 8:172–180.

Gillette MU. 1986. The suprachiasmatic nuclei: circadian phase-shifts induced at the time of hypothalamic slice preparation are preserved in vitro. Brain Res 379:176–181.

Gillette MU. 1991. SCN electrophysiology in vitro: Rhythmic activity and endogenous clock properties. In: Klein DC, Moore RY, Reppert SM, editors, Suprachiasmatic Nucleus: The Mind's Clock, New York, NY: Oxford University Press. pp 125–143.

Glass L, Mackey MC. 1998. From Clocks to Chaos: The Rhythms of Life. Princeton, NJ: Princeton University Press. pp 98–118.

Green DJ, Gillette R. 1982. Circadian rhythm of firing rate recorded from single cells in the rat suprachiasmatic brain slice. Brain Res 245:198–200.

Grehl S, Viola H, Fuller P, Carter KW, Dunlop S, Hool L, Sherrard R, Rodger J. 2015. Cellular and molecular changes to cortical neurons following low intensity repetitive magnetic stimulation at different frequencies. Brain Stimul 8:114–123.

Grehl S, Martina D, Goyenvalle C, Deng ZD, Rodger J, Sherrard RM. 2016. In vitro magnetic stimulation: A simple stimulation device to deliver defined low intensity electromagnetic fields. Front Neural Circuits 10:85.

Huynh W, Vucic S, Krishnan AV, Lin CS, Kiernan MC. 2016. Exploring the evolution of cortical excitability following acute stroke. Neurorehabil Neural Repair 30:244–257.

Kimiskidis VK, Koutlis C, Tsimpiris A, Kälviäinen R, Ryvlin P, Kugiumtzis D. 2015. Transcranial magnetic stimulation combined with eeg reveals covert states of elevated excitability in the human epileptic brain. Int J Neural Syst 25:1550018.

Li W, Yang Y, Ye Q, Yang B, Wang Z. 2007. Effect of chronic and acute low-frequency repetitive transcranial magnetic stimulation on spatial memory in rats. Brain Res Bull 71:493–500.

Lowrey PL, Takahashi JS. 2011. Genetics of circadian rhythms in mammalian model organisms. Adv Genet 74:175–230.

Lu M, Ueno S. 2017. Comparison of the induced fields using different coil configurations during deep transcranial magnetic stimulation. PLoS One 12:e0178422.

Ly JQM, Gaggioni G, Chellappa SL, Papachilleos S, Brzozowski A, Borsu C, Rosanova M, Sarasso S, Middleton B, Luxen A, Archer SN, Phillips C, Dijk D-J, Maquet P, Massimini M, Vandewalle G. 2016. Circadian regulation of human cortical excitability. Nature Comm 7:11828.

Massimini M, Ferrarelli F, Esser SK, Riedner BA, Huber R, Murphy M, Peterson MJ, Tononi G. 2007. Triggering sleep slow waves by transcranial magnetic stimulation. Proc Natl Acad Sci USA 104:8496–8501.

Pascual-Leone A, Tormos JM, Keenan J, Tarazona F, Cañete C, Catalá MD. 1998. Study and modulation of human cortical excitability with transcranial magnetic stimulation. J Clin Neurophysiol 15:333–343.

Paxinos G, Franklin KBJ. 2004. The Mouse Brain in Stereotaxic Coordinates, London: Academic Press. pp 33–38.

Pittendrigh CS, Daan S. 1976. A functional analysis of circadian pacemakers in nocturnal rodents. J Comp Physiol 106:223–252.

Ripperger JA, Albrecht U. 2012. The circadian clock component PERIOD2: From molecular to cerebral function. In: Kalsbeek A, Merrow M, Roenneberg T, Foster RG, editors, The Neurobiology of Circadian Timing—Progress in Brain Research, 199:Amsterdam: Elsevier. pp 233–245.

Rossini PM, Burke D, Chen R, Cohen LG, Daskalakis Z, Di Iorio R, Di Lazzaro V, Ferreri F, Fitzgerald PB, George MS, Hallett M, Lefaucheur JP, Langguth B, Matsumoto H, Miniussi C, Nitsche MA, Pacual-Leone A, Paulus W, Rossi S, Rothwell JC, Siebner HR, Ugawa Y, Walsh V, Ziemann U. 2015. Noninvasive electrical and magnetic stimulation of the brain, spinal cord, roots and peripheral nerves: Basic principles and procedures for routine clinical and research application. An updated report of an I.F.C.N. Committee. Clin Neurophysiol 126:1071–1107.

Rotenberg A, Muller PA, Vahabzadeh-Hagh AM, Navarro X, López-Vales R, Pascual-Leone A, Jensen F. 2010. Lateralization of forelimb motor evoked potentials by transcranial magnetic stimulation in rats. Clin Neurophysiol 121:104–108.

Savelyev SA, Larsson KC, Johansson AS, Lundkvist GBS. 2011. Slice preparation, organotypic tissue culturing and luciferase recording of clock gene activity in the suprachiasmatic nucleus. J Vis Exp 48:e2439.

Siebner H, Rothwell J. 2003. Transcranial magnetic stimulation: New insights into representational cortical plasticity. Exp Brain Res 148:1–16.

Siebner HR, Bergmann TO, Bestmann S, Massimini M, Johansen-Berg H, Mochizuki H, Bohning DE, Boorman ED, Groppa S, Miniussi C, Pascual-Leone A, Huber R, Taylor PC, Ilmoniemi RJ, De Gennaro L, Strafella AP, Kähkönen S, Klöppel S, Frisoni GB, George MS, Hallett M, Brandt SA, Rushworth MF, Ziemann U, Rothwell JC, Ward N, Cohen LG, Baudewig J, Paus T, Ugawa Y, Rossini PM. 2009. Consensus paper: combining transcranial stimulation with neuroimaging. Brain Stimul 2:58–80.

Smeal RM, Ermentrout GB, White JA. 2010. Phase-response curves and synchronized neural networks. Philos Trans Royal Soc B 365:2407–2422.

Stoppini L, Buchs PA, Muller D. 1991. A simple method for organotypic cultures of nervous tissue. J Neurosci Methods 37:173–182.

Tang AD, Hong I, Boddington LJ, Garrett AR, Etherington S, Reynolds JN, Rodger J. 2016. Low-intensity repetitive magnetic stimulation lowers action potential threshold and increases spike firing in layer 5 pyramidal neurons in vitro. Neuroscience 335:64–71.

Tang AD, Bennett W, Hadrill C, Collins J, Fulopova B, Wills K, Bindoff A, Puri R, Garry MI, Hinder MR, Summers JJ, Rodger J, Canty AJ. 2018. Low intensity repetitive transcranial magnetic stimulation modulates skilled motor learning in adult mice. Sci Rep 8:4016.

van der Werf YD, Altena E, van Dijk KD, Strijers RL, De Rijke W, Stam CJ, van Someren EJ. 2010. Is disturbed intracortical excitability a stable trait of chronic insomnia? a study using transcranial magnetic stimulation before and after multimodal sleep therapy. Biol Psychiatry 68:950–955.

Vyazovskiy VV, Olcese U, Lazimy YM, Faraguna U, Esser SK, Williams JC, Cirelli C, Tononi G. 2009. Cortical firing and sleep homeostasis. Neuron 63:865–878.

Welsh DK, Yoo SH, Liu AC, Takahashi JS, Kay SA. 2004. Bioluminescence imaging of individual fibroblasts reveals persistent, independently phased circadian rhythms of clock gene expression. Curr Biol 14:2289–2295.

Yamazaki S, Numano R, Abe M, Hida A, Ri Takahashi, Ueda M, Block GD, Sakaki Y, Menaker M, Tei H. 2000. Resetting central and peripheral circadian oscillators in transgenic rats. Science 288:682–685.

Yang X, Song L, Liu Z. 2010. The effect of repetitive transcranial magnetic stimulation on a model rat of Parkinson's disease. Neuroreport 21:268–272.

Yoo SH, Yamazaki S, Lowrey PL, Shimomura K, Ko CH, Buhr ED, Siepka SM, Hong HK, Oh WJ, Yoo OJ, Menaker M, Takahashi JS. 2004. Period2::Luciferase real-time reporting of circadian dynamics reveals persistent circadian oscillations in mouse peripheral tissues. Proc Natl Acad Sci USA 101:5339–5346.

Yoshikawa T, Yamazaki S, Menaker M. 2005. Effects of preparation time on phase of cultured tissues reveal complexity of circadian organization. J Biol Rhythms 20:500–512.